Energy xxx (2015) 1–7

Contents lists available at ScienceDirect

Energy

journal homepage: www.elsevier.com/locate/energy

MOF-derived Cu/nanoporous carbon composite and its application for electro-catalysis of hydrogen evolution reaction

Jahan-Bakhsh Raoof [a, *], Sayed Reza Hosseini [b], Reza Ojani [a], Sakineh Mandegarzad [a]

[a] Department of Analytical Chemistry, Faculty of Chemistry, University of Mazandaran, 47416-95447, Babolsar, Iran
[b] Nanochemistry Research Laboratory, Faculty of Chemistry, University of Mazandaran, 47416-95447, Babolsar, Iran

ARTICLE INFO

Article history:
Received 9 April 2015
Received in revised form
16 July 2015
Accepted 9 August 2015
Available online xxx

Keywords:
MOF-199
MOF-derived Cu/nanoporous carbon composite
Direct carbonization
Non-platinum catalyst
Hydrogen evolution reaction

ABSTRACT

In this work, metal-organic framework $Cu_3(BTC)_2$ [BTC = 1,3,5-benzenetricarboxylate] (commonly known as MOF-199 or HKUST-1), is used as porous template for preparation of a Cu/nanoporous carbon composite. The MOF-derived Cu/nanoporous carbon composite (Cu/NPC composite) is synthesized by direct carbonization of the MOF-199 without any carbon precursor additive. The physical characterization of the solid catalyst is achieved by using a variety of different techniques, including XRD (X-ray powder diffraction), scanning electron microscopy, thermo-gravimetric analysis, and nitrogen physisorption measurements. The electrochemical results have shown that the Cu/NPC composite modified glassy carbon electrode (Cu/NPC/GCE) as a non-platinum electrocatalyst exhibited favorable catalytic activity for hydrogen evolution reaction, in spite of high resistance to faradic process. This behavior can be attributed to existence of Cu metal confirmed by XRD and/or high effective pore surface area (1025 $m^2\ g^{-1}$) in the Cu/NPC composite. The electron transfer coefficient and exchange current density for the Cu/NPC/GCE is calculated by Tafel plot at about 0.34 and 1.2×10^{-3} $mAcm^{-2}$, respectively.

1. Introduction

NPC (Nanoporous carbon) materials with high surface areas have been widely applied in many fields such as adsorbents [1], catalyst supports [2], and supercapacitor [3]. The advantageous characteristics of highly porous carbons, including their fast kinetics, high surface area, narrow pore size distribution, high pore volume, and high conductivity, have attracted attention for use as supports for preparation of the electrocatalyst [4–6].

Variety methods have been employed for preparation of carbon materials, including laser ablation [7], electrical arc [8], chemical vapor decomposition [9], and templating [10,11] as well as chemical or physical activation methods [12]. Among them, the template method is an effective way for synthesis of the NPC. Two different template modes, i.e., endotemplate and exotemplate [13], can be distinguished according to function of the template. In the exotemplate case, firstly the nanoporous template is prepared. Then, the NPC is synthesized at two different ways; either with addition [14] or without any carbon precursor [15] upon the template as a porous pattern. Different nanoporous templates are used for preparation of the NPC such as nanoporous silicate (MCM-48, SBA-16 and so on) with addition of different carbon precursors such as sucrose and furfuryl alcohol [16,17].

Another group of nanoporous templates that can be used to prepare of nanoporous carbon are MOFs (metal organic frameworks) [4,15]. The MOF as a new class of porous crystalline materials [18] was used for catalysis, gas storage and separation [19]. The MOF can also be used as a template for synthesis of electrically conducting porous carbon materials. Liu and coworkers [20] for the first time, used porous MOFs for synthesis of the carbon nanomaterials and checked their hydrogen storage capability as well as electrochemical capacitance. Park and coworkers [15] reported fabrication of highly porous carbon adsorbents by carbonizing highly crystalline MOF without any carbon precursors and its application for H_2 storage. Ali Khan et al. [4] synthesized the NPC by direct carbonization of MOF-5 and studied it as a support for preparation of electrocatalyst for ethanol oxidation.

Hydrogen is a future fuel because of its high heat of combustion, and high energy capacity per unit volume as compared with conventional fossil fuels. The combustion products of hydrogen are nearly free from pollution [21]. Therefore, there are many attempts to use different modified electrodes for the HER (hydrogen evolution reaction) [22,23]. Although platinum has a high catalytic

* Corresponding author. Tel.: +98 11 35302392; fax: +98 11 35302350.
E-mail address: j.raoof@umz.ac.ir (J.-B. Raoof).

http://dx.doi.org/10.1016/j.energy.2015.08.013
0360-5442/

activity for the HER, limited reserve in earth and high cost restricts its wide application in industry which is a major challenge for commercialization of the device [24]. Therefore, many efforts were made to find the other materials for HER to replace or reduce the use of Pt [25,26].

Herein, we have used $Cu_3(BTC)_2$[BTC = Benzene-1,3,5-tricarboxylate]also known as HKUST-1 (or MOF-199) as a template for fabrication of highly Cu species/nanoporous carbon composite (Cu/NPC composite) by direct carbonization without any carbon precursors at 900 °C. The MOF-199 is one of the most cited MOFs because it has a large surface area, high pore volume, high chemical stability, and easy synthesis. In this structure, each Cu ion is coordinated by four oxygen atoms of benzene-1,3,5-tricarboxylate ligands and by one H_2O molecule that forms dimeric Cu (II) paddlewheel units [27]. The resulting framework is a cubic structure with two types of pores [28]. We have exploited the above mentioned structural characteristics of the MOF-199 and Cu/NPC composite as a catalyst in HER. The results demonstrated that the pore characteristics of the Cu/NPC composite and presence of copper metal catalyst have strongly affected the electrocatalyst activity rather than bare glassy carbon electrode. To the best of our knowledge, this is the first report on synthesis of the Cu/NPC composite and its application for use in HER in acid medium.

2. Experimental

2.1. Materials

H_3BTC (Benzene-1,3,5-tricarboxylic acid, 95%) was acquired from Aldrich. $Cu(NO_3)_2.3H_2O$, 99.99% and ethanol as solvent were supplied by Fluka. All reagents were of analytical grade and used without further purification. Solutions were made with twice distilled water.

2.2. Preparation of the CU/NPC composite

Porous MOF-199 was prepared by using a hydrothermal method based on the reported procedure [29]. In the typical synthesis, $Cu(NO_3)_2 \cdot 3H_2O$ (2.327 g) was dissolved into 25 mL of deionized water. The above process was followed by addition of H_3BTC (1.414 g) in 50 mL of solvent consisting of equal parts of ethanol and deionized water and mixed thoroughly until it was completely dissolved. The solution was stirred for 15 min. The resultant solution was transferred into a 250 mL Teflon-lined stainless steel autoclave. It was kept at 423 K in an isothermal oven for 15 h, yielding light blue crystals. After cooling the autoclave to room temperature, the solid product was filtered and washed several times by ethanol and water. The product was then dried at 423 K. The Cu/NPC composite catalyst was prepared by direct carbonization of the MOF-199 during followed producer as similar to the previously reported [4]. In the typical synthesis, dried MOF-199 was transferred to a ceramic boat. The boat was placed in a quartz tube which is fixed in a tube furnace (Nabertherm B 180). Air was evacuated by continuous flow of N_2 for 30 min, and temperature of the furnace was raised to 550 °C to polymerization of the MOF-199 [1]. Further carbonization was performed at 900 °C under N_2 atmosphere for 6 h. The Carbon product was denoted as Cu/NPC composite.

2.3. Characterization

XRD (X-ray powder diffraction) patterns were recorded on a Philips 1830 diffractometer using Cu-K_α radiation source, 0.05 step size and 1s step over the range of $4° < 2\theta < 90°$. The BET (Brunauer–Emmett–Teller) surface areas of the samples were determined by means of N_2 adsorption at 77 K using micrometrics model ASAP2010 sorptometer. Prior to N_2 adsorption, the samples were evacuated at 473 K under vacuum. The surface area was determined from the liner part of the famous BET equation. The pore size distribution was calculated using BJH (Barrett–Joyner–Halenda) method. Surface morphology and percent composition of the catalyst was examined by using a scanning electron microscope (Philips XL-30) combined with EDS (energy-dispersive X-ray Spectroscopy) machine. The samples were coated with gold in order to increase their conductivity before scanning. TGA (Thermo-gravimetric analysis) was used to determine the thermal stability of the synthesized materials and was carried out from room temperature to 873 K by using a TGA (Mettler Toledo 851) analyzer at a heating rate of 10 K/min under N_2 atmosphere.

2.4. Electrode preparation and electrochemical performance test

Electrochemical characterization was performed in a conventional three-electrode cell. A Ag|AgCl|KCl (3 M) and a platinum wire served as reference and counter electrodes, respectively. To prepare of working electrode (Cu/NPC/GCE), 1.5 mg of the as-prepared catalyst was suspended in 1 mL of ethanol by ultrasonic bath for 15 min. Then, 7 μL of this mixture (without adding any binder and conductive agents) were deposited onto the glassy carbon electrode (GCE, 2 mm in diameter), which was previously polished with alumina powder (0.3 μm) and cleaned in the pure ethanol sonicately and washed with distillated water. As the same method, MOF-199/GCE was prepared for comparative investigations. Electrochemical techniques, such as cyclic voltammetry, linear sweep voltammetry for the HER, chronoamperometry and electrochemical impedance spectroscopy were performed by using a potentiostat/galvanostat (SAMA 500-C Electrochemical analysis system, Sama, Iran) coupled with a personal computer. Electrochemical impedance spectroscopy was performed by an Autolab model PGSTAT 30 with FRA software version 4.9 (Eco Chemie, Netherlands).

3. Result and discussion

3.1. Characterization of the synthesized materials

Characterization of the MOF-199 and Cu/NPC composite compounds usually involves XRD (structure identification), SEM analysis (morphology), N_2 adsorption–desorption isotherm (textural properties of surface area/pore volume), and TGA (structural stability). Fig. 1a exhibits the XRD pattern for the MOF-199. The main diffraction peaks at $2\theta = 9.4°$, 11.62°, 17.4°, 19°, 29.3° and relative diffraction intensities of MOF-199 were found to be the same as previous report [29]. After direct carbonization of this template as shown in Fig. 1b, the XRD pattern represents all the main peaks which are attributed to Cu metal (with highest intensity), CuO, and Cu_2O deriving from decomposition of the MOF-199 template. It was discriminated that the Cu is major element after carbonization at 900 °C, because this temperature is lower than the boiling point of Cu (up to 2000 °C). Thus, Cu presented in the decomposed MOF-199 cannot be removed by N_2 flow and it is loaded on the Cu/NPC composite.

The SEM image of the MOF-199 was frequently displayed crystals which look pyramidal in shape (Fig. 2a, b), and the particle size is about 10–20 μm. The SEM image was taken after carbonization of the porous template as shown in Fig. 2c, d. As can be seen in this figure, the pyramidal crystalline was disturbed due to carbonization at 900 °C. The spherical nanoparticles were observed that was assembled in cauliflower-like structure. Also, as shown in trace d, the nanoparticle size of the Cu/NPC composite at about 20 nm was

Please cite this article in press as: Raoof J-B, et al., MOF-derived Cu/nanoporous carbon composite and its application for electro-catalysis of hydrogen evolution reaction, Energy (2015), http://dx.doi.org/10.1016/j.energy.2015.08.013

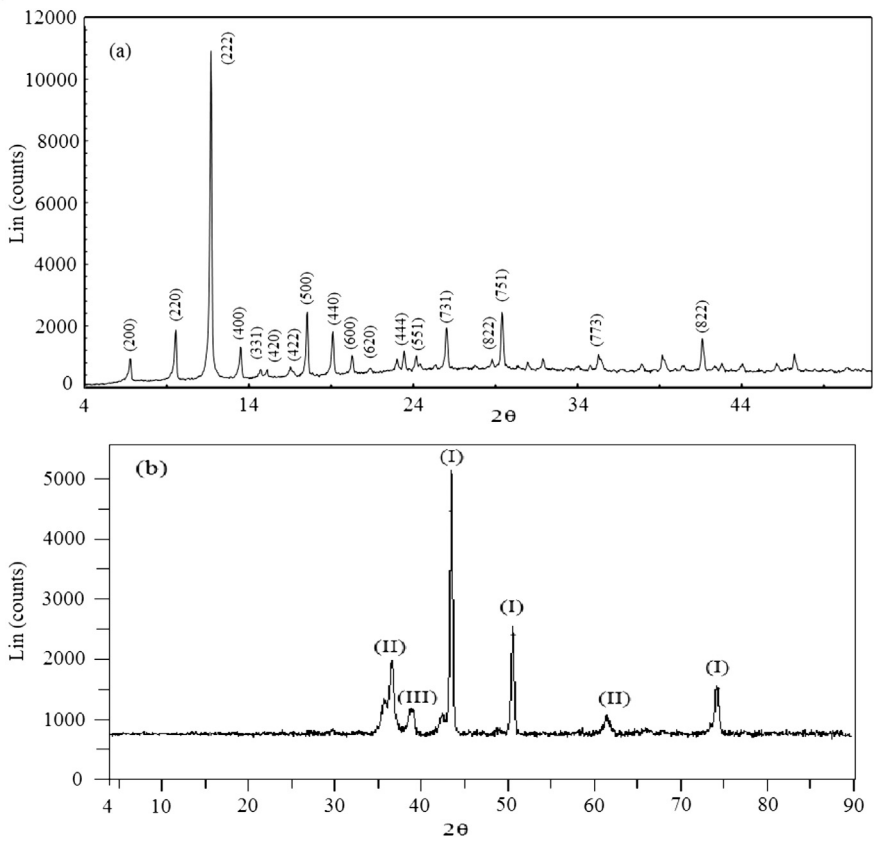

Fig. 1. XRD pattern of (a) MOF-199 and (b) Cu/NPC composite. In Fig. 1b, (I), (II), and (III) indicate the peak position of the Cu, Cu_2O and CuO, respectively.

smaller than the MOF-199. Therefore, it is anticipated that the external surface area that attributed to particle size was increased duo to decreasing of particle size in the Cu/NPC composite.

To study the bulk composition of the MOF-199 and Cu/NPC composite in more details, EDS analysis was performed (Fig. 3). The EDS spectra display that the MOF-199 and Cu/NPC composite structures contain C and Cu. The specimens were coated with an ultra-thin coating of gold.

Thermal stability of the MOF-199 was checked by the TGA curve at N_2 atmosphere (Fig. 4). The result demonstrated thermodynamic stability of the materials up to 350 °C. The weight loss was observed at two steps: the first weight loss (22.15%) occurred in the range of 100–200 °C related to loss of the embedded solvent. The second weight loss (46.50%) between 300 °C and 350 °C is corresponding to decomposition of the organic species. According to TGA curve, octahedral framework of the MOF-199 is decomposed at 350 °C and then completely carbonized at higher temperature under N_2 atmosphere.

A nitrogen adsorption/desorption technique was used to determine the surface porous textural properties of the synthesized compounds (Fig. 5). In trace (a), N_2 adsorption isotherm type (I) reflects the microporous network of the MOF-199. In trace (b), the Cu/NPC composite isotherm depicted combined characteristics of (I/IV) IUPAC isotherms that is represented micro-meso structure of the Cu/NPC composite. BET surface area is comprised an internal and external component [30]. External surface area was affected from factors such as completely smooth particle, density, particle diameter. Internal surface area was associated with walls of open pores. It is suggested that the magnitude of internal surface area is a function of varying open pore surface area due to sample preparation condition. Although the increasing of the external surface area was proposed from the SEM pictures, BET pore surface area and pore volume were slightly reduced after carbonization but it was maintained at about 1025 $m^2\ g^{-1}$ which was probably due to filling of pores by the deposited copper during the carbonization process.

Table 1 reported BET surface area (S), total pore volume (V), and pore size (D) of the MOF-199 and Cu/NPC composite. The PSD (pore-size distribution) was derived by using BJH (Barrett–Joyner–Halenda).The PSD of the MOF-199 showed a narrow pore size centered at 1.3 nm (Fig. 6). PSD of the Cu/NPC composite (inset of Fig. 6) depicted a uniform pore size centered at 1.8 nm with negligible mesoporous. These results were proved the micro-meso structure of the Cu/NPC composite.

The CV for the $K_4Fe(CN)_6$ solution at the surface of a bare GCE gave anodic and corresponding cathodic peak of the $Fe(CN)_6^{3-/4-}$ redox system (Fig. 7a). However, Faradaic current was dramatically attenuated once on the Cu/NPC/GCE (trace b) and MOF-199/GCE (trace c), indicating that electron transfer kinetic between the electrode surface and $K_4Fe(CN)_6$ was effectively reduced. It is due to semiconductor properties of the MOF-199 and Cu/NPC composite.

In order to understand the electrochemical behavior of the MOF-199 and Cu/NPC composite materials, electrochemical impedance spectroscopy technique was employed (Fig. 8). It is obvious from this figure that there is an increasing resistive values in the Cu/NPC/GCE rather than the MOF-199/GCE and bare GCE. This difference could be related to the semiconductor properties of the Cu/NPC composite [31]. The resistance to the faradic process at Cu/NPCC is higher than the MOF-199 which is due to the presence of much more Cu_2O in the Cu/NPCC.

Please cite this article in press as: Raoof J-B, et al., MOF-derived Cu/nanoporous carbon composite and its application for electro-catalysis of hydrogen evolution reaction, Energy (2015), http://dx.doi.org/10.1016/j.energy.2015.08.013

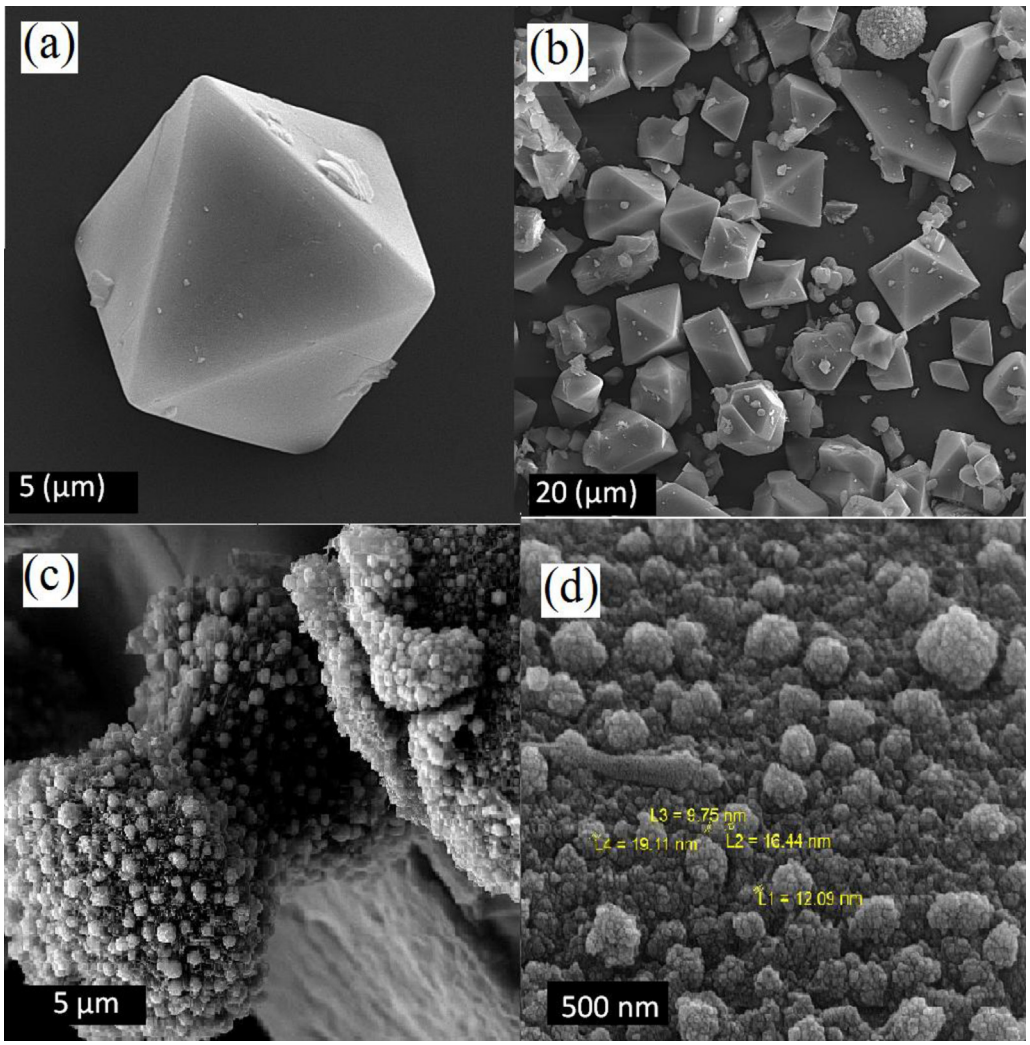

Fig. 2. SEM images of the MOF-199 (a, b) and Cu/NPC composite (c, d).

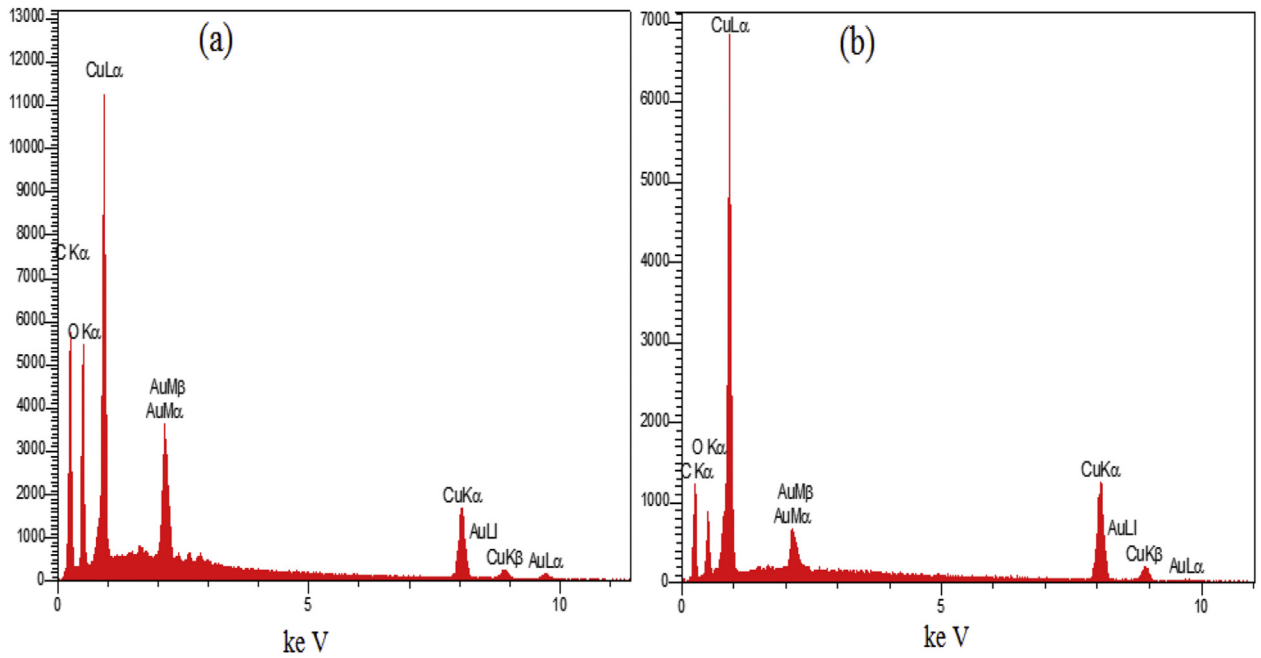

Fig. 3. EDS spectra for the MOF-199 (a) and Cu/NPC composite (b).

Please cite this article in press as: Raoof J-B, et al., MOF-derived Cu/nanoporous carbon composite and its application for electro-catalysis of hydrogen evolution reaction, Energy (2015), http://dx.doi.org/10.1016/j.energy.2015.08.013

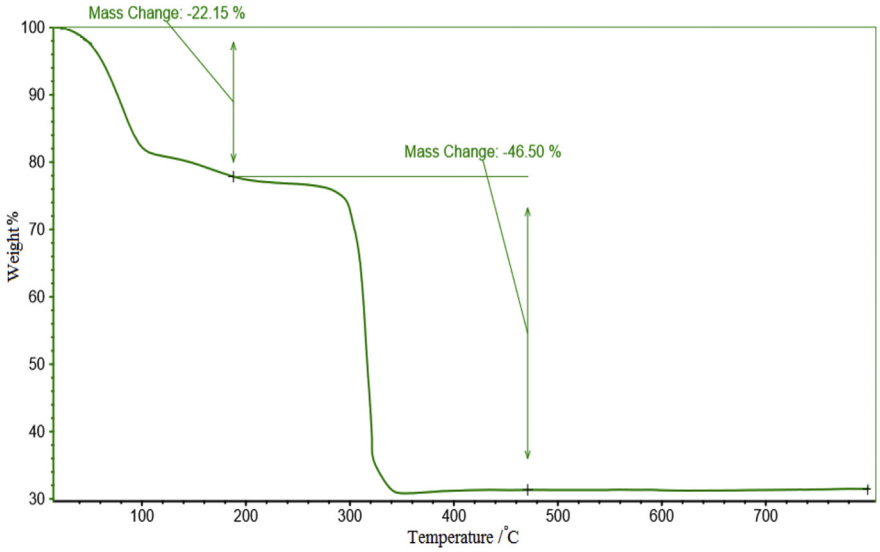

Fig. 4. TGA and DTG curves of the MOF-199.

3.2. Electrochemical properties of the Cu/NPC composite as catalyst for the HER

The electrocatalytic activity of the as-fabricated electrodes for the HER was investigated by LSV technique in 0.5 M H_2SO_4 (Fig. 9). A comparison of the LSVs demonstrates that current density (current normalized per geometric surface area) at potential of −1.0 V for bare GCE and MOF-199/GCE and Cu/NPC/GCE are about −0.546, −1.378, and −10.655 mA cm^{-2}, respectively. This result showed an improvement in comparison with previously reported by Koca [32]. Koca was represented that copper phetalocyanine catalyzed the HER at more negative over potential (−1.0 V vs. SCE) rather than the Cu/NPC composite (over-potential about −0.8 V vs. Ag|AgCl|KCl (3 M)). As shown in this figure, the MOF-199 is several orders less active than that the Cu/NPC composite towards HER. In the MOF-199, copper as catalyst is strongly involved at framework and it forms covalence coordination bond with BTC ligand in 3D structure [31], thus it is expected that the weaker catalysis activity. After carbonization and decomposition of the MOF-199, copper is existed in form of Cu metal, CuO and Cu_2O with the higher activity rather than the MOF-199. As can be seen, the slope of current density-potential curve for the Cu/NPC/GCE as non platinum catalyst is steeper than bare GCE and the its over-potential at $j = -0.54$ mA cm^{-2} is about 200 mV lower than that the bare GCE. Furthermore, possessing good surface area and expected hydrogen adsorption properties of the Cu/NPC composite can probably cause an improvement of the HER catalysis. This is inference of previously literature that a high hydrogen adsorption property was reported for MOF-5/derived nanoporous carbon [15].

Kinetic analysis of the HER was performed and pertaining Tafel plots were constructed in Fig. 10 from current density-potential

Table 1
BET surface areas (S), pore volumes (V) and pore sizes (D) for the synthesized samples.

Sample	S (m^2 g^{-1})	V[a] (cm^3 g^{-1})	D[b] (nm)
MOF-199	1370	0.573	1.67
Cu/NPC composite	1025	0.479	1.87

[a] The pore volume is calculated at a relative pressure of 0.97.
[b] The pore diameter is referred to the pore size corresponding to the peak position in Fig. 6.

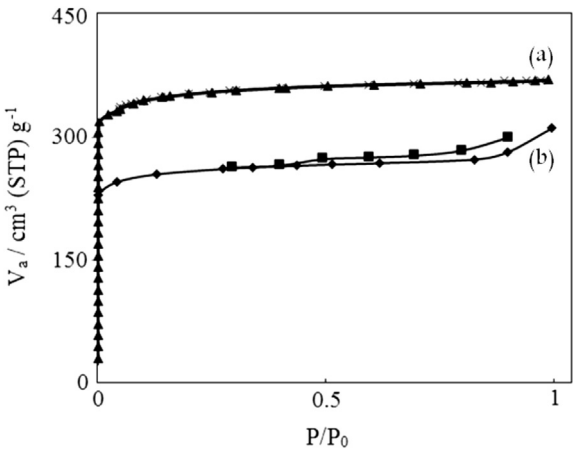

Fig. 5. Nitrogen adsorption–desorption isotherms of the MOF-199 (a) and Cu/NPC composite (b). The (◆, ▲) and (■, ×) symbols refer to adsorption and desorption branches, respectively.

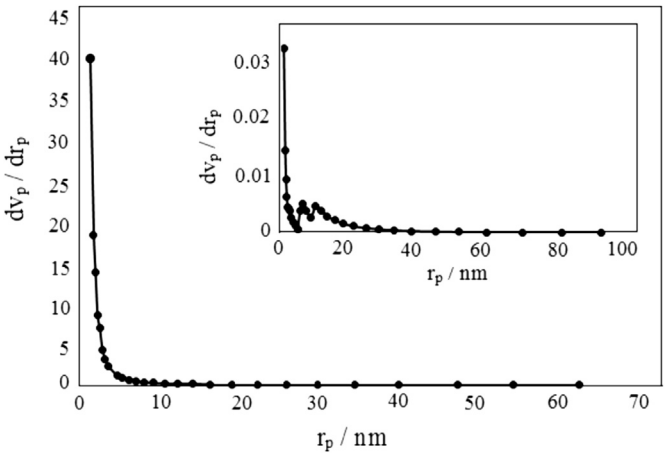

Fig. 6. PSD of the MOF-199. Inset: PSD of the Cu/NPC composite.

Please cite this article in press as: Raoof J-B, et al., MOF-derived Cu/nanoporous carbon composite and its application for electro-catalysis of hydrogen evolution reaction, Energy (2015), http://dx.doi.org/10.1016/j.energy.2015.08.013

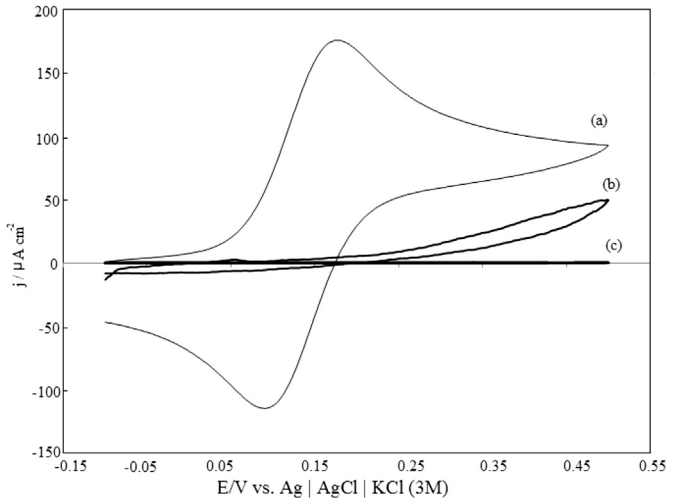

Fig. 7. Cyclic voltammetry of 1.0 mM $K_4Fe(CN)_6$ in 0.1 M KCl solution at a bare GCE (a), Cu/NPC/GCE (b) and MOF-199/GCE (c) at $\nu = 50$ mV s^{-1}.

data in the voltammograms recorded at Fig. 9. Tafel slopes and exchange current densities (j_0) were calculated by means of the least-squares analysis of the plots. The value of j_0 for the Cu/NPC composite catalyst is about 4 times higher than the bare GCE (Table 2). This means that catalytic activity of the GCE is enhanced when the Cu/NPC composite material is loaded on its surface. As reported earlier [33], cathodic transfer coefficient ($\alpha \approx 0.5$) describes a mechanism where the rate is controlled by the discharge step, independent of the nature of hydrogen recombination. In our work, α value was obtained 0.34, confirming a mechanism for the HER where the rate is probably controlled by the discharge step.

In addition, the long-term stability of the Cu/NPC/GCE for the HER was investigated with chronoamperogram recorded at −0.9 V in 0.5 M H_2SO_4 (Fig. 11). The result indicates that the current does not drop significantly to 0.5 h.

4. Conclusion

A novel metal organic framework-derived Cu/NPC composite was successfully synthesized via direct carbonization of the MOF-199 as template at 900 °C under N_2 atmosphere without addition of carbon source. The obtained Cu/NPC composite was exhibited cauliflower-like morphology with particle size about 20 nm. It consisted of Cu metal, CuO, Cu_2O according to XRD result. This material was showed a good surface area and micro-meso structure. Electrochemical measurements of the Cu/NPC/GCE indicate improvement of HER catalysis in the more positive onset potential and higher current density rather than bare GCE. This enhancement is attributed to both of existent of Cu, CuO, and Cu_2O in the Cu/NPC composite structure, good surface area, and expected hydrogen adsorption properties of the Cu/NPC composite. It is suggested that

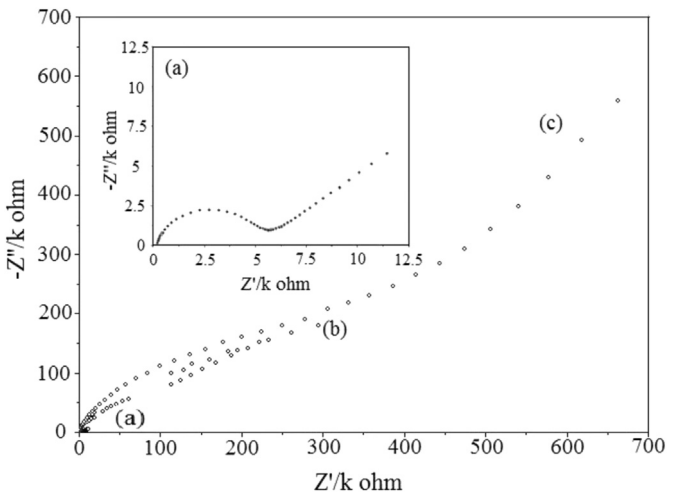

Fig. 8. Nyquist plot for the Faradaic impedance measurements performed at the surface of (a) bare GCE, (b) MOF-199/GCE and (c) Cu/NPC/GCE. The measurements were performed in the presence of a 1.0 mM solution of $K_3[Fe(CN)_6]/K_4[Fe(CN)_6]$ 1:1 mixture upon biasing the working electrode at 0.2, 0.18, 0.19 V for the GCE, MOF-199/GCE, and Cu/NPC/GCE, respectively.

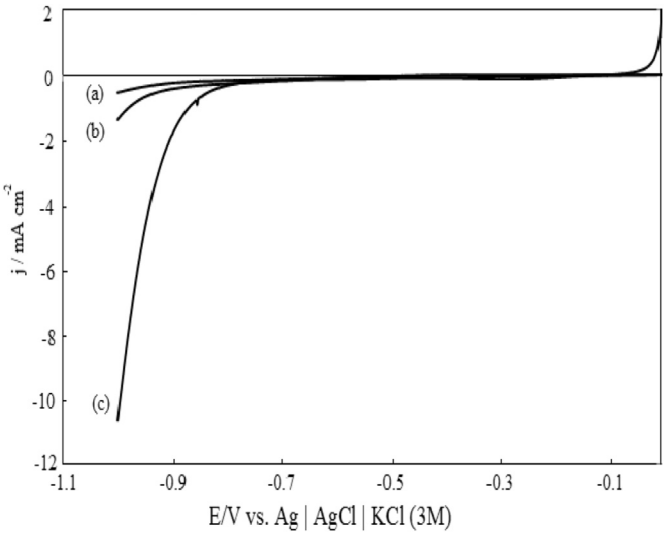

Fig. 9. LSVs for the HER on (a) bare GCE, (b) MOF-199/GCE and (c) Cu/NPC/GCE in 0.5 M H_2SO_4 solution at $\nu = 10$ mV s^{-1}.

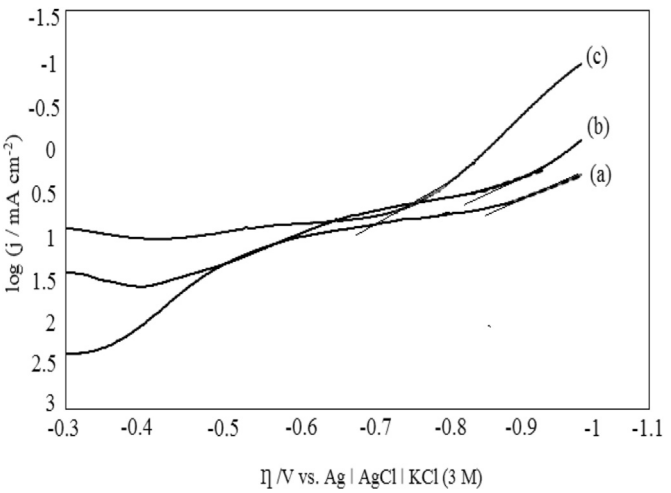

Fig. 10. Tafel plots for the HER in 0.5 M H_2SO_4 solution at (a) bare GCE, (b) MOF-199/GCE, and (c) Cu/NPC/GCE.

Table 2
Tafel parameters for the HER.

Electrode	-log (j_0, mA cm^{-2})	j_0 (× 10^{-4}mAcm^{-2})	Slop (V^{-1} dec^{-1})	α
Bare GCE	3.60	2.5	3.03	0.17
MOF-199/GCE	3.07	9.2	3.33	0.19
Cu/NPC/GCE	2.99	10.2	5.69	0.34

Please cite this article in press as: Raoof J-B, et al., MOF-derived Cu/nanoporous carbon composite and its application for electro-catalysis of hydrogen evolution reaction, Energy (2015), http://dx.doi.org/10.1016/j.energy.2015.08.013

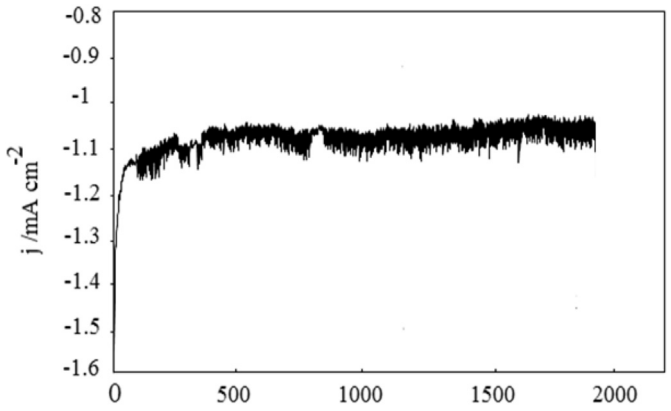

Fig. 11. Chronoamperogram for the HER catalyzed by the Cu/NPC/GCE at −0.9 V in 0.5 M H_2SO_4 solution.

the MOF-199 was probably converted to a NPC which was deposited copper metal that it is cheaper than the platinum catalysts.

References

[1] Yang SJ, Kim T, Im JH, Kim YS, Lee K, Jung H. MOF derived hierarchically porous carbon with exceptional porosity and hydrogen storage capacity. J Mater Chem 2012;24:464–70.
[2] Calvillo L, Celorrio V, Moliner R, Garcia AB, Caméan I, Lazaro MJ. Comparative study of Pt catalysts supported on different high conductive carbon materials for methanol and ethanol oxidation. Electrochim Acta 2013;102:19–27.
[3] Lee SY, Kim JI, Park SJ. Activated carbon nanotubes/polyaniline composites as supercapacitor electrodes. Energy 2014;78:298–303.
[4] Ali Khan I, Badshah A, Haider N, Ullah S, Anjum DH, Nadeem MA. Porous carbon as electrode material in direct ethanol fuel cells (DEFCs) synthesized by the direct carbonization of MOF-5. Solid State Electrochem 2014;18:1545–55.
[5] Anbia M, Mandegarzad S. Enhanced hydrogen sorption on modified MIL-101 with Pt/CMK-3 by hydrogen spillover effect. J Alloys Compd 2012;532:61–7.
[6] Maiyalagan T, Nassr ABA, Alaje TO, Bron M, Scott K. Three-dimensional cubic ordered mesoporous carbon (CMK-8) as highly efficient stable Pd electrocatalyst support for formic acid oxidation. J Power Sources 2012;211:147–53.
[7] Thess A, Lee R, Nikolaev P, Dai H, Petit P, Robert J. Crystalline ropes of metallic carbon nanotubes. Science 1996;273:483–7.
[8] Journet C, Maser WK, Bernier P, Loiseau A, Chapelle ML, Lefrant S. Large-scale production of single-walled carbon nanotubes by the electric-arc technique. Nature 1997;388:756–8.
[9] Zhao F, Vicenzo A, Hashempour M, Bestetti M. Supercapacitor electrodes by direct growth of multi-walled carbon nanotubes on Al: a study of performance versus layer growth evolution. Electrochim Acta 2014;150:35–45.
[10] Lee SY, Kim BJ, Park SJ. Influence of H_2O_2 treatment on electrochemical activity of mesoporous carbon-supported Pt–Ru catalysts. Energy 2014;66:70–6.
[11] Yang SJ, Kim T, Lee K, Kim YS, Yoon J, Park CR. Solvent evaporation mediated preparation of hierarchically porous metal organic framework-derived carbon with controllable and accessible large-scale porosity. Carbon 2014;71:294–302.
[12] Ahmadpour A, Do DD. The preparation of active carbons from coal by chemical and physical activation. Carbon 1996;34:471–9.
[13] Wu X, Hong X, Luo Z, Hui KS, Chen H, Wu J, et al. The effects of surface modification on the supercapacitive behaviors of novel mesoporous carbon derived from rod-like hydroxyapatite template. Electrochim Acta 2013;89:400–6.
[14] Liu B, Shioyama H, Jiang H, Zhang X, Xu Q. Metal–organic framework (MOF) as a template for syntheses of nanoporous carbons as electrode materials for supercapacitor. Carbon 2010;48:456–63.
[15] Yang SJ, Kim T, Im JH, Kim YS, Lee K, Jung H, et al. MOF-derived hierarchically porous carbon with exceptional porosity and hydrogen storage capacity. J Mater Chem 2012;24:464–70.
[16] Stojmenović M, Momčilović M, Gavrilov N, Pašti IA, Mentus S, Jokić B, et al. Incorporation of Pt, Ru and Pt-Ru nanoparticles into ordered mesoporous carbons for efficient oxygen reduction reaction in alkaline media. Electrochim Acta 2015;153:130–9.
[17] Farzinnejad N, Shams E, Bennett JC. Ordered mesoporous carbon CMK-5 as a potential sorbent for fuel desulfurization: application to the removal of dibenzothiophene and comparison with CMK-3. Micropor Mesopor Mater 2013;168:239–46.
[18] Yaghi OM, O'Keeffe M, Ockwig NW, Chae HK, Eddaoudi M, Kim J. Reticular synthesis and the design of new materials. Nature 2003;423:705–14.
[19] Langmi HW, Ren J, North B, Mathe M, Bessarabov D. Hydrogen storage in metal-organic frameworks: a review. Electrochim Acta 2014;128:368–92.
[20] Liu B, Shioyama H, Akita T, Xu Q. Metal-organic framework as a template for porous carbon synthesis. J Am Chem Soc 2008;130:5390–402.
[21] Ojani R, Valiollahi R, Raoof JB. Comparison between graphene supported Pt hollow nanospheres and graphene supported Pt solid nanoparticles for hydrogen evolution reaction. Energy 2014;74:871–6.
[22] Ojani R, Hasheminejad E, Raoof JB. Hydrogen evolution assisted electrodeposition of bimetallic 3D nano/micro-porous Pt Pd films and their electrocatalytic performance. Int J Hydrogen Energy 2014;39:8194–203.
[23] Yin Z, Chen F. A facile electrochemical fabrication of hierarchically structured nickel-copper composite electrodes on nickel foam for hydrogen evolution reaction. J Power Sources 2014;265:273–81.
[24] Vijh AK. The chemical approach to the properties determining the dielectric strength of gaseous materials. J Mater Chem 1979;4:51–66.
[25] Kiani A, Hatami S. Fabrication of platinum coated nanoporous gold film electrode: a nanostructured ultra-low platinum loading electrocatalyst for hydrogen evolution reaction. Int J Hydrogen Energy 2010;35:5202–9.
[26] Raoof JB, Ojani R, Kiani A, Rashid-Nadimi S. Fabrication of highly porous Pt coated nanostructured Cu-foam modified copper for hydrogen evolution reaction. Int J Hydrogen Energy 2010;35:452–8.
[27] Chui SSY, Lo SMF, Charmant JPH, Orpen AG, Willis IDA. Chemically functionalizable nanoporous material $[Cu_3\ (TMA)\ _2(H_2O)\ _3]\ _n$. Science 1999;283:1148–50.
[28] Krakiew P, Kramer M, Sabo M, Kunschke R, Frmde H, Kaskel S. Improved hydrogen storage in the metal-organic framework $Cu_3(BTC)_2$. Adv Eng Mater 2006;8:293–6.
[29] Xiang ZH, Cao DP, Shao XH, Wang WC, Zhang JW, Wu WZ. Facile preparation of high-capacity hydrogen storage metal organic frameworks: a combination of microwave-assisted solvothermal synthesis and supercritical activation. Chem Eng Sci 2010;65:3140–6.
[30] Hodson ME. Measurements of internal and external surface area in feldspars implications for mineral dissolution studies. Mineral Mag 1998;62A:634–5. Goldschmidt Conference Toulouse.
[31] Loera-Serna S, Oliver-Tolentino MA, López-Núñez MDL, Santana-Cruz A, Guzmán-Vargas A, Cabrera-Sierra R. Electrochemical behavior of $[Cu_3(BTC)_2]$ metal-organic framework: the effect of the method of synthesis. J Alloys Compd 2012;540:113–20.
[32] Koca A. Copper phthalocyanine complex as electrocatalyst for hydrogen evolution reaction. Electrochem Commun 2009;11:838–41.
[33] Ojani R, Raoof JB, Hasheminejad E. One-step electroless deposition of Pd/Pt bimetallic microstructures by galvanic replacement on copper substrate and investigation of its performance for the hydrogen evolution reaction. Int J Hydrogen Energy 2013;38:92–9.

Please cite this article in press as: Raoof J-B, et al., MOF-derived Cu/nanoporous carbon composite and its application for electro-catalysis of hydrogen evolution reaction, Energy (2015), http://dx.doi.org/10.1016/j.energy.2015.08.013